Identification of the Q_Y Excitation of the Primary Electron Acceptor of Photosystem II: CD Determination of Its Coupling Environment

Nicholas Cox,*,† Joseph L. Hughes,†,‡ Ronald Steffen,† Paul J. Smith,† A. William Rutherford,†,‡ Ron J. Pace,† and Elmars Krausz†

Research School of Chemistry, Australian National University, Canberra, ACT 0200, Australia, and iBiTec-S, CNRS URA 2096, Bât 532, CEA Saclay, 91191 Gif-sur-Yvette, France

Received: October 5, 2008; Revised Manuscript Received: July 7, 2009

Low-temperature absorption and CD spectra, measured simultaneously, are reported from Photosystem II (PS II) reduced with sodium dithionite. Spectra were obtained using PS II core complexes before and after photoaccumulation of $Pheo_{D1}^-$, the anion of the primary acceptor. For plant PS II, $Pheo_{D1}^-$ was generated under conditions in which the primary plastoquinone was present as an anion (Q_A^-) and as a modified species taken to be the neutral doubly reduced hydroquinone (Q_AH_2). The bleaches observed upon $Pheo_{D1}^-$ formation in the presence of Q_A^- are shifted to the blue compared those in the presence of Q_AH_2. This is attributed to the influence of the charge on Q_A^-, and this effect mirrors the well-known electrochromic effect of Q_A^- on the neutral pigments. The absorption bleaches induced by $Pheo_{D1}$ reduction are species dependent. Structured changes of the CD in the 680−690 nm spectral region are seen upon photoaccumulation of $Pheo_{D1}^-$ in PS II from plant, *Synechocystis* and *Thermosynechococcus vulcanus.* These CD changes are shown to be consistent with the overall electronic assignments of Raszewski et al. [Raszewski et al. *Biophys. J.* **2008**, *95*, 105], which place the dominant $Pheo_{D1}$ excitation near 672 nm. CD changes associated with $Pheo_{D1}$ reduction are modeled to arise from the shift and intensity changes of two CD features: one predominately of Chl_{D1} character, the other predominately $Pheo_{D2}$ in character. The assignments are also shown to account for the Q_Y absorption changes in samples where the quinone is its charged (Q_A^-) and neutral (Q_AH_2) states.

Introduction

Photosystem II (PS II), a pigment−protein complex found in higher plants, algae, and cyanobacteria, is responsible for the catalytic conversion of water to molecular oxygen in oxygenic photosynthesis. Its core contains the D1 and D2 reaction center polypeptides that bind the redox-active centers involved in charge separation and water oxidation.

Charge separation in PS II occurs upon excitation of P680, a chlorophyll assembly bound to both D1 and D2 protein subunits, resulting in the transfer of an electron to the neighboring $pheo_a$ ($Pheo_{D1}$) and subsequently to plastoquinone cofactors (Q_A and Q_B). Electrons that re-reduce $P680^+$ come from the oxygen-evolving complex (OEC) via the redox-active tyrosine residue 161 (Y_Z) of the D1 protein. The OEC, which is the substrate water-binding site of the PS II protein, is then in turn re-reduced by electrons from the oxidation of water (for review, see ref 1).

Chemical Reduction of PS II. Several chemical treatments have been identified in PS II that allow the electron transfer pathway to be poised in intermediate states. Treatment of PS II with the strong reducing agent, sodium dithionite, at pH 7 reduces the plastoquinone Q_A and cyt_{b559} in the dark.[2−4] Subsequent illumination at <200 K leads to the stable reduction of the primary electron acceptor $Pheo_{D1}$, with $P680^+$ being re-reduced by the cyt_{b559}.[2−4] The $Pheo_{D1}^-$-Q_A^- state has a distinctive EPR split signal, and this resonance was first observed in nonoxygenic photosynthetic bacterial reaction centers (BRCs), which are structurally and functionally homologous to the reaction center of PS II.

Sustained illumination of dithionite-treated PS II above 270 K leads to further modification of the quinone (Q_A). This was proposed to be the charge-neutral quinol (Q_AH_2) form, because of the disappearance of the characteristic semiquinone-iron signal,[2,5] and when the iron is in the low spin form, the loss of the semiquinone EPR signal.[6] In this case, when the $Pheo_{D1}$ is photoreduced its EPR signal is a simple radical ($g \sim 2.003$, p−p 15 G) rather than a split signal,[4,5] consistent with the formation of the diamagnetic Q_AH_2 state. In the current report, we refer to the form of Q_A following this treatment as the Q_AH_2 state, since this is the most likely protonation configuration for the double reduced state, though evidence for this form is circumstantial (see van Mieghem et al.[7]).

Assignments of the Electronic Excitations of the $Pheo_{D1}$ and Chl_{D1}. Klimov et al.[8] first reported the optical consequence of photoinduced reduction of $Pheo_{D1}$ in dithionite-treated PS II. Two bleaches were observed in the illuminated-minus-dark spectrum of the chlorin Q_X-Q_Y region at 545 nm (fwhm ∼ 4 nm) and 683 nm (fwhm ∼2 nm). The bleach pattern generated in PS II was similar to the absorption spectrum of $Pheo_a$ in solution,[9] although significantly red-shifted. The Q_X and Q_Y bleach positions correlated well with the two known electrochromic shifts induced by the formation of Q_A^-.[10]

The change in linear dichroism upon photoaccumulation[11] of $Pheo_{D1}$ indicated two components within the bleach in the Q_Y region. The main bleach component at 683 nm was accompanied by what was attributed to a shift of a chl_a pigment near 680 nm. The orientations of the transition dipoles for the Q_X bleach and main Q_Y bleach component were found to be parallel and

* Corresponding author. Email address: cox@mpi-muelheim.mpg.de. Telephone: +61-2-6125-3577; Fax: +61-2-6125-8997.
† Australian National University.
‡ CNRS URA 2096.

10.1021/jp808796x CCC: $40.75
Published on Web 08/17/2009

perpendicular to the membrane plane, respectively. This is consistent with conventionally assigned orientations of the transition dipoles[12−14] of $Pheo_{D1}$ using recent crystallographic results.[15]

Mutagenesis has identified that the Q_X bands for $BPheo_L$ in the BRC[16] and for $Pheo_{D1}$ in PS II from *Synechocystis*[17] red shift due to a hydrogen bond to the 13^1 keto ring substituent. This hydrogen bond also induces a red shift of the main Q_A^--induced shift feature in the Q_Y region in the PS II mutants from *Synechocystis*.[17] The Q_A^--induced electrochromism of the BRC mutants[16] has not been reported. However, the absorption and linear dichroism[18] suggest that the $BPheo_L$ Q_Y band blue shifts due to this hydrogen bond, and we note that there is minimal effect on the other pigments. Thus, by influencing the $BPheo_L$ or $Pheo_{D1}$ the effects on the optical spectra appears to be dominated by the shift of a single band.

The strong structural and functional similarity between the electron acceptor sides of PS II and the BRC makes the Q_Y and Q_X assignment of the $Pheo_{D1}$ discussed above difficult to reconcile. In the BRC, the Q_A^--induced electrochromism of the $BPheo_L$ bands for Q_Y and Q_X is consistent with a conventional assignment of the $\Delta\mu$ vectors being approximately in-line with the $BPheo_L$ molecular *y*- and *x*-axes. This leads to a $\sim$100 cm^{-1} red shift of the Q_Y band and a negligible shift on the Q_X band.[19,20] Conversely, in PS II there is a large blue shift of $Pheo_{D1}$ Q_X (the C550 shift),[10,21] and no readily discernible large red shift in Q_Y.[13,22]

To reconcile this anomaly, an unconventional $\Delta\mu$ orientation for $Pheo_{D1}$ has been proposed.[22] This places $\Delta\mu_X$ aligned perpendicular to the membrane plane and $\Delta\mu_Y$ parallel to the plane.

Recent Models for PSII Electronic Structure. Detailed consideration of optical lineshapes has recently led to the development of theoretical models for the electronic structure of the PSII reaction center.[14,23−25] As input for these models, exciton coupling values for the reaction center pigments were estimated on the basis of structural data,[15,26] followed by a global evolutionary fitting procedure to a wide range of optical data. From this approach, site energies for the reaction center pigments were estimated as well as the exciton states of the reaction center.

Raszewski et al. fit absorption-difference data for $Pheo_{D1}$ photoinduced reduction[23] and Q_A^- electrochromism.[14] In this modeling, neither the main bleach upon $Pheo_{D1}$ photoinduced reduction nor the main Q_A^--induced electrochromism feature directly identify the $Pheo_{D1}$ position. There are three salient features arising from this model:

(i) The $Pheo_{D1}$-Chl_{D1} dipole−dipole coupling is $\sim$50 cm^{-1}.

(ii) The lowest energy pigment transition is predominantly localized on Chl_{D1}, at $\sim$682 nm in D1/D2/cyt_{b559}[23] and $\sim$685 nm in core complexes.[14]

(iii) The exciton transition that is dominated by the $Pheo_{D1}$ absorption appears at $\sim$672 nm in both D1/D2/cyt_{b559} and core preparations.[14,23] This is at significantly shorter wavelength than suggested by earlier photoinduced reduction and mutagenesis studies, as discussed above ($\sim$684 nm in PSII core complexes).

In the recent modeling of Novoderezhkin et al.,[24,25] a charge-transfer state involving the P_{D1}-P_{D2} pigments is included. Charge transfer states are not included in the model of Raszewski et al.[14,23] In the Novoderezhkin et al. model,[24,25] the lowest energy exciton transition ($\sim$681 nm) is dominated by Chl_{D1} but includes other reaction center pigments. In this treatment, $Pheo_{D1}$ contributes significantly to all the delocalized reaction center excitations. However, Novoderezhkin et al.[24,25] do not include $Pheo_{D1}$ photoinduced reduction data or Q_A^--induced electrochromism data in their analysis.

Experimental Test of the Current Acceptor Side Model. In this study, we directly examine the question as to where $Pheo_{D1}$ predominantly absorbs. This allows experimental estimation of the maximum coupling strength between this pigment and Chl_{D1} and assignment of the dominant Q_Y feature in the Q_A^- induced electrochromic pattern. We present new spectral data, taking advantage of the improved resolution available by optical measurements taken at 1.7 K and our ability to measure CD (Abbreviations: CD, circular dichroism; EPR, electron paramagnetic resonance; PS II, Photosystem II; BRC, bacterial reaction center; Q_A, primary plastoquinone A acceptor of PS II; chl_a, chlorophyll$_a$; $pheo_a$, pheophytin$_a$; $cytb_{559}$, cytochrome b_{559}; fwhm, full width at half-maximum) as well as accurate absorption spectra simultaneously. Specifically, we address the following: (i) absorption changes associated with photoinduced reduction of $Pheo_{D1}$ with the quinone as either Q_A^- or Q_AH_2; (ii) corresponding CD changes; and (iii) the species dependence of the above absorption and CD changes.

Materials and Methods

Preparation of Spinach Core Complexes. PS II core complexes from spinach were made according to the method of Smith et al.[27] The cores displayed activity of $\sim$2500−4000 μmol O_2 per mg chl/h and were stored at 1−3 mg chl_a/mL in 400 mM sucrose, 20 mM NaCl, 2 mM $MgCl_2$, and 0.3 g/L DDM, pH 6.5 at 88 °C until use. *Synechocystis* sp. strain PCC 6803 (*Synechocystis*) cores were provided by R. Debus.[28] *Thermosynechococcus vulcanus* (*T. vulcanus*) cores were provided by J.-R. Shen.[29,30]

Dark Reduction of Q_A to Q_A^-. Reduction of Q_A to Q_A^- was achieved by adding sodium dithionite to a 1 mg chl_a/mL aqueous suspension of a PS II core complex in the dark. Dithionite solutions (1 M HEPES, pH 7.0 (HCl)) were prepared 1−2 min prior to use. A $\sim$2 μL volume of this dithionite solution was added to $\sim$20 μL of PS II sample in an Eppendorf tube. This solution was rapidly introduced into an optical cell,[31] which was then attached to the sample rod and transferred to the cryostat. The sample was frozen to 4 K over a time period of $\sim$40 s. The time taken to complete the entire procedure was 2−3 min. The final concentration of dithionite in the sample containing the PS II was $\sim$6 mg/mL.

Double Reduction of Q_A to Q_AH_2. Double reduction to form the Q_AH_2 state was performed on samples initially reduced to the Q_A^- state (see above). After chemical treatment with sodium dithionite to form the Q_A^- state and introduction into optical cells, but prior to freezing, samples were illuminated for $\sim$5 min at room temperature (285 K) and then allowed to relax for 1 h in the dark in an O_2-free (gaseous He) atmosphere. Samples were then frozen to 4 K.

Photoinduced Reduction of $Pheo_{D1}^-$ in either the Q_A^- or Q_AH_2 "Dark" State. Photoinduced reduction of the $Pheo_{D1}$ state was achieved by visible illumination with either an Ar^+ laser or halogen lamp. All low-temperature illuminations (1.7 K) of the PS II core complex samples used the argon laser. The laser was tuned to 514 nm, with output of 300 mW/cm^2 at the sample. Illuminations were typically 15−20 min in length. High-temperature (285 K), white light illuminations used a 150 W quartz halogen lamp imaged onto the sample through a 10 cm water heat filter for $\sim$1 min.

Optical Sample Protocols. The PS II preparation was diluted with a 1:1 (v/v) mix of ethylene glycol and glycerol as a glassing agent. The final concentration of this glassing agent was 40%

v/v. This liquid sample was introduced into a strain-free, quartz-windowed cell assembly[31] with path length of 200 μm and mounted on a sample rod. The rod was inserted into an Oxford Instruments Spectromag 4 cryostat, through a helium gas lock, the latter fitted with quartz observation/illumination windows. The lock provided an anaerobic environment for room-temperature illumination. To achieve glasses of good quality, the sample rod was plunged into liquid helium. Absorption and CD data were collected simultaneously on a custom-built spectrometer designed in our laboratory.[32] It employed a 0.75 m Spex Czerny-Turner single monochromator using a 1200 lines/mm grating blazed at 500 nm, with dispersion of 1.1 nm/mm.

Q_X Fitting. A simultaneous fitting of all $pheo_a$ Q_X data was undertaken (see Figure 7A−E). This data included (i) the $pheo_a$ eo Q_X absorption profile (in both Q_A and Q_A^- states); (ii) the $Pheo_{D1}^-$ bleach (in both Q_A^- and Q_AH_2 states); and (iii) the electrochromic pattern induced by the reduction of Q_A.

A least-squares minimization routine was employed to find the optimal solution. This fitting assumed the oscillator strength for both $pheo_a$ Q_X transitions to be the same. The line shape of each $pheo_a$ transition ($Pheo_{D1}$ and $Pheo_{D2}$) was approximated by the sum of two Gaussians. Both Gaussians describing the $Pheo_{D1}$ were broadened by a factor of 1.5 to fit the $Pheo_{D1}$ bleach data in the Q_AH_2 state (Figure 7D). For a complete description of the fitting procedure, see the Discussion and Supporting Information s4.

Simulations of the Q_Y Exciton Scheme. Simple exciton calculations were undertaken for the PS II originating from different species in order to simultaneously fit the CD difference and absorption difference spectra upon $Pheo_{D1}$ reduction. Our approach is based on the model of Raszewski et al.,[14] which we evaluate on the basis of our new data on core complexes. The six core pigments of the reaction center were included in the calculation. Charge transfer states were not included. The coupling matrix of Raszewski et al.[14] was used. Here, excitonic couplings between the reaction center pigments were calculated using the ab initio TrEsp method (see Raszewski et al.[14]). These calculations were based on the recent 3.0 Å crystal structure of PS II.[15] The coupling matrix is given in the Supporting Information s5. Transition dipole moments were taken to be 4.4 D for chl_a and 3.4 D for $pheo_a$ as per Raszewski et al.[14]

For the calculation of the difference spectra, the absorbance and CD spectra were calculated twice, first with all pigments present and second without the $Pheo_{D1}$. Electrochromic shifts of the transition energies of the remaining pigments were accounted for as described in Raszewski et al.[23] In this work, the electrochromic shifts induced by Q_A^- and $Pheo_{D1}^-$ were estimated at three different $\Delta\mu_Y$ orientations: 0°, 13°, and 18° off the N_B-N_D axis toward N_C (see Supporting Information s5). All three angles gave approximately the same result. Simulations presented in the text assume a $\Delta\mu$ orientation for all pigments to be ~18° off the N_B-N_D axis toward N_C.

The homogeneous line shapes of the optical transitions were not calculated. These were considered to have only a relatively small influence on the estimated profile of the inhomogeneous absorption bands. As in Raszewski et al. 2008,[14] static disorder in optical transitions was taken into account in our simulations. All pigment site energies were assumed to have a Gaussian distribution. (see Supporting Information s5 and s6). The mean site energies for the six reaction center pigments were varied, starting with the values used by Raszewski et al.[14,23] so as to account for the D1/D2/$cytb_{559}$ data reported in Krausz et al.[33] It was found that it was necessary to shift the site energies of the pigment transitions only slightly (<60 cm^{-1}) to reproduce the 2 K absorption profile. This shift is attributed to the fact that the simplified calculations presented here did not include the effects of electron−phonon coupling, which would manifest itself in a homogeneous component to the absorption band shape. Simulations reported here reproduced the absorption, CD, and $Pheo_{D1}$ bleach data of D1/D2/$cytb_{559}$ reaction centers reasonably well. This is shown in the Supporting Information s5.

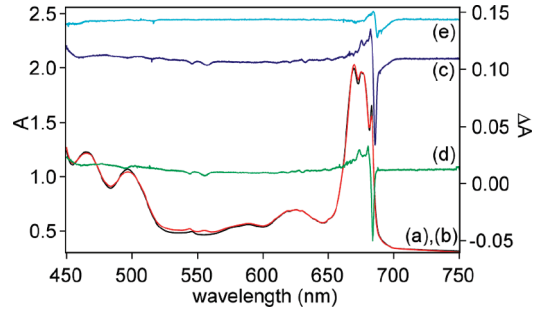

Figure 1. Absorption spectra of untreated (a, black) and dithionite-treated (b, red) spinach cores. Illuminated-minus-dark difference spectra of the dithionite-treated sample; (c, blue) after 1.7 K, 514 nm illumination, 300 mW/cm^2 for 20 min, (d, green) following annealing at 90 K (2−5 min); (e, cyan) the change induced by annealing (i.e., (d) − (c)).

The site energies obtained from the D1/D2/cyt_{b559} data were then further adjusted as necessary to fit the core complex data. The mean site energy of the Chl_{D1} was shifted to lower energy (~100 cm^{-1}) and its site distribution narrowed (Δ_{inh} ~50 cm^{-1}). A similar modification to the Chl_{D1} pigment site energy/distribution was used in fitting PS II core complex data (see Raszewski et al.[14]). In addition, the mean site energy of the $Pheo_{D2}$ was shifted to lower energy (~100 cm^{-1}) to rationalize the structured CD difference.

Results

Plant PS II Core Complexes. ***Absorption Spectra of PS II Cores Following $Pheo_{D1}^-$ Photoaccumulation in the Q_A^- State.*** Figure 1 shows the absorption spectrum of an untreated (trace (a), black) and dithionite-treated (trace (b), red) PS II spinach core complex sample over the 450−750 nm region. The addition of dithionite in the dark (see Materials and Methods) reduced Q_A and $cytb_{559}$, as is known from earlier work.[2,4] The reduced form of cyt_{b559} gave rise to a new band at 555.6 nm reviewed in Stewart et al.,[34] which is shown in detail in Figure 2.

Electronic excitations of the quinone (Q_A) do not appear in the visible region.[10,21] The redox state of the quinone can, however, be inferred via its electrostatic influence on surrounding pigment absorptions, particularly via the well-known "C550" electrochromic shift on the Q_X $pheo_a$ excitation (544.0 nm).[10,21] This band shifts 2−3 nm to the blue as a consequence of the photoinduced formation of Q_A^-. An identical band shift was observed in the (dark) absorption spectrum of chemically reduced PS II core complexes.[31] Apart from the C550 shift, little overall change was seen in the absorption spectrum compared to that of untreated PS II core complexes. This establishes that there has been no chemical reduction or major change in electronic structure of the PS II core pigment assembly upon dithionite treatment (also see Supporting Information Figure S1).

Illumination of dithionite reduced PS II spinach core complexes at 1.7 K yielded stable bleaches at 544.0, 555.6, and 683.8 nm as identified in traces (c,d) in Figure 1 and Figure 2. The bleaches at 544.0 and 555.6 nm correspond to the loss of $Pheo_{D1}$[8] and $cytb_{599}^{red}$, respectively. The overall spectral changes in the chlorin Q_Y region were close to conservative, i.e., such

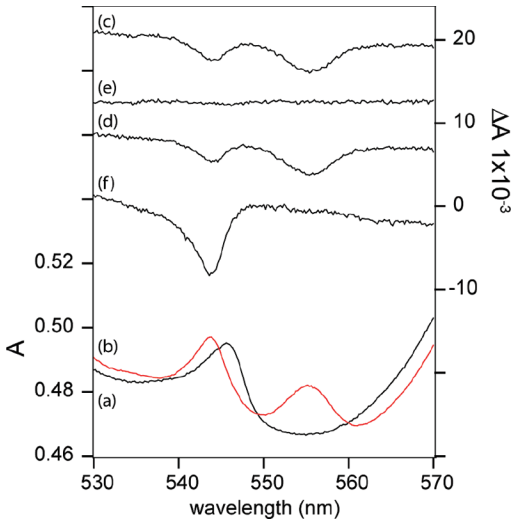

Figure 2. Detail of Figure 1 in the Q_X region (a−d) as Figure 1, with (f) difference spectrum after white light illumination at 285 K, performed on a second sample.

that the negative and positive absorption changes balance, with no net change in absorption. Most notable is the apparent narrow bleach at 683.8 nm (fwhm 2 nm). Positive absorption changes (665−680 nm) include features at 672 and 680 nm. Similar absorption changes were induced upon 285 K illumination. Their magnitude is ∼5× larger than the 2 K bleach (see Supporting Information, Figure S2).

Annealing the sample at 90 K for 2−5 min led to the reversal of a broad derivative pattern in the Q_Y region (trace (e) Figure 1) without a measurable change in the Q_X region (trace (e) Figure 2). Therefore, these conservative changes in absorption occurred under conditions where no reoxidation of $Pheo_{D1}^-$ occurred. We attributed the changes in Q_Y upon annealing to reversible photophysical processes associated with the CP43/CP47 proximal antennae subunits that are analogous to the spectral changes seen in isolated CP43.[35,36] All quantifications of $Pheo_{D1}$ bleaching determined in the current work was made on data from samples annealed to 90 K.

Control EPR measurements were made in conjunction with the optical measurements to clearly identify the redox state of the quinone in the dark reduced samples. In nonilluminated samples, the $g \sim 1.9$ Q_A^--Fe^{2+} signal[2] was observed, but no $cytb_{559}^{ox}$ signal (see Supporting Information Figure S3A). Low-temperature illumination (<200 K) generated a split signal (∼50 G) previously assigned in both PS II[2,4] and nonoxygenic bacterial reaction centers (BRCs)[37] to the interaction of the $Pheo_{D1}$ anion ($S = 1/2$) with the antiferromagnetically coupled Q_A^--Fe^{2+} ($S = 5/2$) complex (see Supporting Information Figure S3B).

Quantification of $Pheo_{D1}^-$ Formation in the Q_A^- State: $cytb_{559}$ as the Electron Donor at 1.7 K. The degree of $Pheo_{D1}$ reduction induced by 1.7 K illumination can be deduced from the area of the 544.0 nm Q_X bleach, relative to the area of the original Q_X absorption. Illumination at 1.7 K bleached ∼10% of the entire Q_X $pheo_a$ band (i.e., 20% of $Pheo_{D1}$). $Cytb_{559}$ oxidation can be calculated in the same way. Approximately 20% of the $cytb_{599}$ absorption was lost upon 1.7 K illumination. The two signals scale quantitatively, and thus, the process can be described as formation of the $Pheo_{D1}^-$-$cytb_{559}^{ox}$ radical pair. Illumination at 285 K (trace (f), Figure 2) led to loss of absorption equal to one $pheo_a$ (i.e., 100% of $Pheo_{D1}$). We did not detect the oxidation of $cytb_{559}$ under these conditions. Any oxidized $cytb_{559}$ was presumably rereduced by the excess

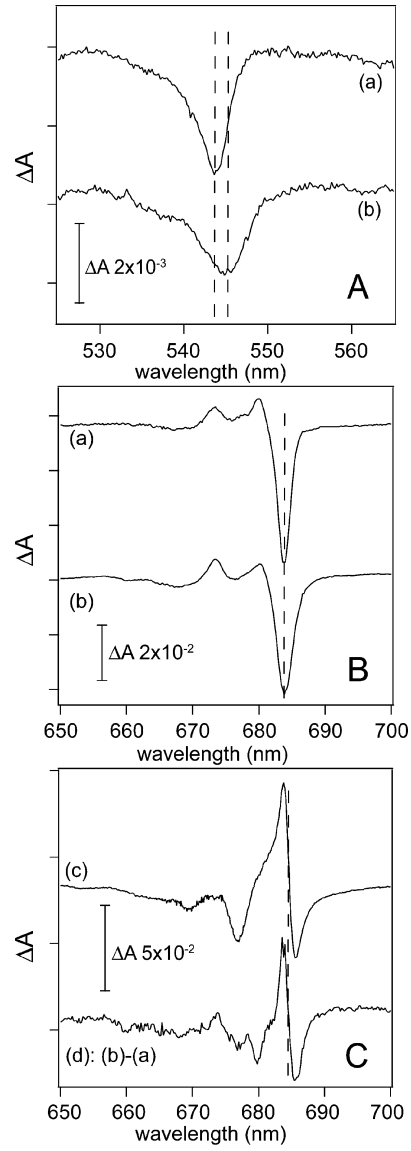

Figure 3. Illuminated-minus-dark difference spectra following photoaccumulation $Pheo_{D1}^-$ in Q_A^- and Q_AH_2 forms of spinach PS II cores. Panel A: Q_X region (a) Q_A^-, (b) Q_AH_2. Panel B as Panel A Q_Y region. Panel C: (c) reference electrochromic shift pattern observed upon 1.7 K photo-induced reduction of Q_A in untreated PS II spinach cores; (d) (b) − (a) of Panel B (see text). The spectra are scaled to the same pre-illumination absorbance in Q_Y.

dithionite. A description of this quantification, including the procedure used to establish an appropriate baseline, is given in the Supporting Information (Figure S4).

The apparent narrow bleach (fwhm 2 nm) centered at 683.8 nm accounts for a loss of absorbance of ∼0.5 ± 0.1% of the total chlorin Q_Y region (650−700 nm). This absorbance envelope consists of ∼33 chl_a and 2 $pheo_a$ molecules per PS II core complex.[27] Thus, the area of the bleach corresponds to a 25 ± 5% loss of $pheo_a$, assuming the $pheo_a$ oscillator strength is 0.7 of one chl_a.[38] Hence, the apparent narrow Q_Y bleach is in excess of what could be attributed to the actual $Pheo_{D1}$ bleach, as quantified by Q_X, by up to 50%. The bleach thus cannot be readily described as absorption loss associated with an isolated $pheo_a$. Illumination at 285 K generated a bleach of ∼5× greater area (see Supporting Information Figure S2).

Comparison of $Pheo_{D1}^-$ Formation in the Q_A^- and Q_AH_2 States. Panels A and B of Figure 3 compare the illuminated-minus-dark difference spectra for PS II prepared from spinach

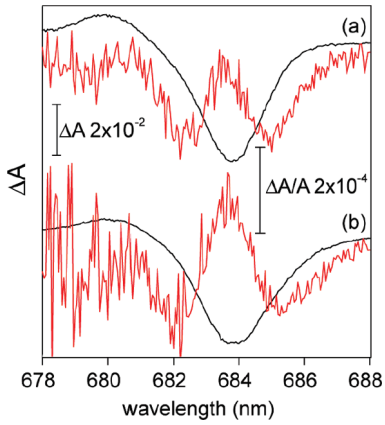

Figure 4. Illuminated-minus-dark CD difference spectra (red traces) following photoaccumulation $Pheo_{D1}^-$ in Q_A^- and Q_AH_2 forms of spinach PS II cores at 1.7 K, traces (a) and (b), respectively. The CD changes are superimposed on the corresponding absorption changes (black traces, see Figure 3). Illumination conditions as per Figure 1.

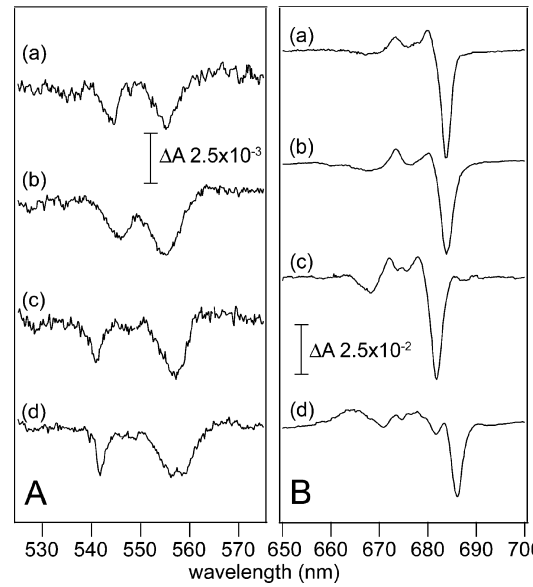

Figure 5. Illuminated-minus-dark difference spectra following photoaccumulation $Pheo_{D1}^-$ at 1.7 K in the Q_X (panel A) and Q_Y (panel B) regions for (a) spinach (Q_A^-), (b) spinach (Q_AH_2), (c) *Synechocystis*, and (d) *T. vulcanus* PS II cores. Bleach spectra include a 90 K annealing to remove photophysical artifacts (see text). Illumination conditions as per Figure 1.

with charged (Q_A^-) or neutral (Q_AH_2) forms of the primary quinone acceptor. In both samples, 1.7 K illumination leads to $cytb_{559}$ acting as the sole terminal electron donor. The Q_X bleach position is shifted 2−3 nm to the red in the Q_AH_2 state (trace (b) panel A Figure 3) compared to the bleach in the Q_A^- state (trace (a) panel A Figure 3). This is consistent with the $Pheo_{D1}$ no longer experiencing the electrochromic influence of the anion, Q_A^-. The Q_Y bleach in the Q_AH_2 state broadens to ∼3 nm fwhm and undergoes a small (∼0.1−0.2 nm) red shift when compared to the bleach in the Q_A^- state (Figure 3 panel B). Apart from these shifts, the bleach patterns in both states are very similar.

The shift in the Q_Y region is more readily observed in the double difference spectrum in Figure 3 panel C, trace (d). Here, the Q_A^- illuminated-minus-dark difference is subtracted from the Q_AH_2 difference (Figure 3, panel B, traces (a) and (b), respectively). This subtraction in Q_Y yields a derivative feature corresponding to the main feature in the electrochromic shift pattern, with precisely the same 684.5 nm crossing point. If the Q_Y bleach position were merely broadened in the Q_AH_2 state, a second differential shape would be observed in the double difference spectrum. The derivative feature seen in the double difference spectrum of Figure 3C has ∼60−70% of the peak-to-peak amplitude of the large feature seen in the electrochromic pattern of untreated PS II. Some of this reduction can be attributed to an increase in the inhomogeneous broadening evident in the apparent Q_Y bleach observed in the Q_AH_2 state.

EPR measurements on PS II samples in the relaxed Q_AH_2 state showed no Q_A^--Fe^{2+} resonance, i.e., after 285 K illumination and a 1 h dark relaxation of the sample at 285 K (see Supporting Information Figure S3A). Low-temperature illumination did not generate the split signal that is characteristic of the $Pheo_{D1}^-$-Q_A^- state, but two other signals were observed. A ^3P signal[39] was seen under illumination at 5 K and a stable isolated radical centered at $g \sim 2.003$ with a peak-to-peak spacing of 15 G was accumulated (see Supporting Information Figure S3C).

CD Changes upon $Pheo_{D1}^-$ Formation. The CD spectra of a dithionite-treated spinach core complex and of untreated samples are very similar (see Supporting Information Figure S1). This further indicates that the electronic structure of the PS II pigments has not changed significantly. The CD change associated with $Pheo_{D1}$ reduction is not only structured, but the net area change (Figure 4) is not consistent with the CD of chl_a or $pheo_a$ as isolated pigments. With the sign and magnitude of the CD of monomeric chl_a or $pheo_a$ as reported ($\Delta A/A \sim -1.5 \times 10^{-4}$),[38] the net change in CD, seen in Figure 4, when scaled for the fractional $Pheo_{D1}$ bleach (∼20%) is the opposite sign and 4−5× larger than the CD of monomeric pigments.

The CD change near 683.8 nm appeared as a structured feature, with components narrower than the absorption depletion seen at this wavelength. An analogous change in CD that is 5× larger was observed upon 285 K illumination, where complete reduction of $Pheo_{D1}$ was achieved (Supporting Information Figure S2). The CD changes that were observed for samples poised in the Q_A^- or Q_AH_2 forms were very similar. The CD change observed here in intact PS II core complexes isolated from spinach is significantly different from an earlier study using D1/D2/$cytb_{559}$ preparations isolated from pea.[40] It is unclear whether this difference represents real species variation between spinach and peas or is intrinsic to the two different types of PS II preparations. This is addressed in more detail in Krausz et al.[33]

Species Comparison of $Pheo_{D1}^-$ Photoaccumulation. ***Absorption Changes upon $Pheo_{D1}^-$ Formation at 1.7 K.*** The illuminated-minus-dark spectra observed upon 1.7 K photoinduced reduction of the $Pheo_{D1}$ in PS II from higher plant (for Q_A^- and Q_AH_2 forms) and cyanobacteria (Q_A^- form) were similar (Figure 5). The spectra of the Q_X region demonstrate that $Pheo_{D1}$ reduction occurs, and they were used to quantify that $cytb_{559}$ acts as the sole electron donor at 1.7 K. Systematic differences between species are seen in the positions of the Q_X band (see also Peterson Årsköld et al.[22]) and in the positions of the narrow Q_Y bleach. We compare first the results for spinach and *Synechocystis* and then discuss *T. vulcanus.*

The $Pheo_{D1}$ fraction that is photobleached is the same in plant as in *Synechocystis*, when monitored by Q_X (∼20%). The same mismatch in integrated intensity of Q_X and the apparent Q_Y bleach was observed. The apparent narrow Q_Y bleach is in excess of what could be attributed to the actual $Pheo_{D1}$ bleach, as quantified by Q_X, by up to 50%. All difference spectra are close to conservative. For the Q_A^- form, in the Q_Y region the fwhm of the bleaches are 2 and 2.5 nm for spinach and *Synechocystis*,

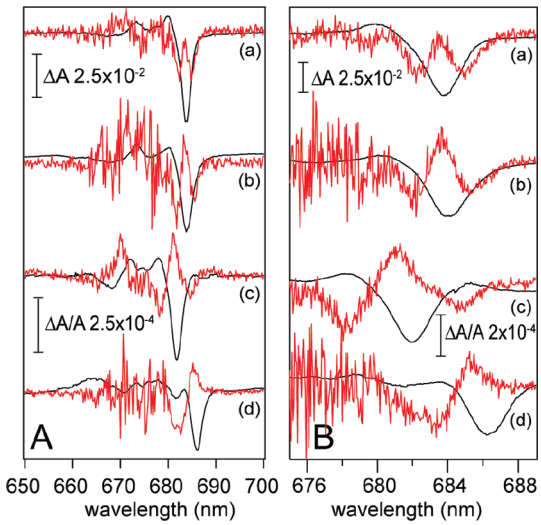

Figure 6. Illuminated-minus-dark CD difference-spectra (red traces) following photoaccumulation $Pheo_{D1}^-$ at 1.7 K in (a) spinach (Q_A^-), (b) spinach (Q_AH_2), (c) *Synechocystis*, and (d) *T. vulcanus* PS II cores. For both panels, black, absorption difference; red, CD difference. CD difference/bleach spectra include a 90 K annealing to remove photophysical contributions (see text). Illumination conditions as per Figure 1.

respectively. The Q_AH_2 form for spinach gave an apparent Q_Y bleach with a fwhm of 3 nm. Positive absorption features in the 665−680 nm region were similar in both species, with notable features at 672 and 680 nm in spinach and 672 and 678 nm in *Synechocystis*. The Q_X and apparent Q_Y bleach positions are blue-shifted in *Synechocystis* compared to spinach.

The bleaches seen in PS II from *T. vulcanus* (Figure 5, trace (d)) retain the key features seen in plant PS II. A narrow (2.5 nm fwhm) apparent Q_Y bleach at 685.8 nm was observed. In *T. vulcanus*, the Q_X bleach was to the blue compared to spinach, as in *Synechocystis*. However, unlike *Synechocystis* the Q_Y bleach for *T. vulcanus* was to the red compared to spinach. The fractional $Pheo_{D1}$ bleach (as estimated from Q_X) corresponded to 10−15% of reaction centers. This is significantly less than the bleach seen in either spinach or *Synechocystis*.

Upon annealing to 90 K, this relatively small $Pheo_{D1}$ Q_X bleach decayed by ∼50%. In other species measured (spinach and *Synechocystis*), the corresponding bleach was stable at 90 K. As a consequence, the bleach spectra reported in Figure 5 trace (d) for *T. vulcanus* is the difference between a spectrum taken immediately after illumination at 2 K and a spectrum taken before illumination. The other species studied were annealed at 90 K to remove photophysical artifacts (see the above section Absorption Spectra of PS II cores following $Pheo_{D1}^-$ photoaccumulation in the Q_A^- state). As with spinach and *Synechocystis*, the net area of the apparent Q_Y bleach near 685 nm overestimated the degree of $Pheo_{D1}$ reduction by up to ∼50%.

CD Changes upon $Pheo_{D1}^-$ Formation at 1.7 K. The CD changes in all the species are very distinctive and appear as structured signals about the narrow absorption bleach features (Figure 6). In all the CD difference spectra, there is a positive lobe approximately in the position of the bleach.

In the 650−680 nm region, there may be some other smaller changes in the CD spectra upon photoinduced $Pheo_{D1}$ reduction, but these are broad and comparable to the noise level. These CD data are shot-noise-limited, which leads to signal-to-noise ratio being somewhat lower in the 650−680 nm region, owing to the higher absorption in this region. Only for *Synechocystis* are there any features of magnitude comparable to the structured changes in the region of the main narrow absorption bleach.

TABLE 1: $Pheo_{D1}$ Absorption Bleach Positions and Corresponding ΔCD Turning Points

	ΔA bleach position (nm)		ΔCD turning point (nm)		
	Q_X	Q_Y	−	+	−
Spinach (Q_A^-)	544.0	683.8	682.4	683.5	685.1
Spinach (Q_AH_2)	545.6	684.0	682.0	683.7	685.4
Synechocystis (Q_A^-)	541.2	681.8	678.2	681.1	684.6
T. vulcanus (Q_A^-)	541.4	685.8	683.3	685.5	-

All bleach positions and CD turning points are summarized in Table 1.

Discussion

Q_X $Pheo_{D1}$ Transition in Higher Plant PS II: Absorption Spectra. A summary of our analysis of the $pheo_a$ Q_X transitions in PS II core complexes from spinach is shown in Figure 7. To extract the $pheo_a$ absorption profile from the data, we performed an iterative baseline correction procedure that required self-consistency within all the data sets presented in Figure 7 (see Supporting Information S4). We present (Figure 7) the baseline-subtracted data and the corresponding fits to (i) the absorption spectra in the Q_A^- and Q_A states (panels A and B), (ii) the bleaches in the Q_A^- and Q_AH_2 states (panels C and D), and (iii) the (Q_A^--minus-Q_A) electrochromic shift (panel E).

A global fit of all the data was made, as described in the Materials and Methods and in the Supporting Information s4. The use of single Gaussians for each $pheo_a$ does not adequately describe the data. The line shapes for each $pheo_a$ were then modeled as a sum of two Gaussians. Equal total areas were attributed to each $pheo_a$. For one of the $pheo_a$ absorption bands, the use of two Gaussians was unnecessary, as the fitting process yielded two bands of equivalent width and position (Q_A^-/Q_AH_2 18477 cm^{-1}, fwhm = 17.0 nm). The other $pheo_a$ band is

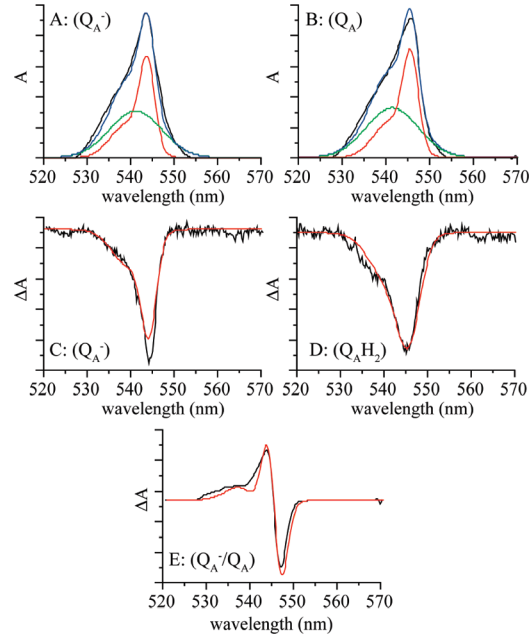

Figure 7. Panel A: Q_X baseline-corrected absorption in the Q_A^- state. Panel B: Q_X baseline-corrected absorption in the Q_AH_2 state. Panel C: 285 K illumination induced bleach in the Q_A^- state. Panel D: 285 K illumination induced bleach in the Q_AH_2 state. Panel E: electrochromic shift induced by Q_A^- formation. For all panels, black, data; red, simulated $Pheo_{D1}$ line shape; green, simulated $Pheo_{D2}$ line shape; blue, simulated $Pheo_{D1}$ + $Pheo_{D2}$ line shape.

dominated by a narrow component (Q_A^-/Q_AH_2 18 386/18 332 cm^{-1}, fwhm = 5.0 nm), with a broader contribution (Q_A^- 18 536/18 481 cm^{-1}, fwhm = 11.2 nm) to higher energy by 150 cm^{-1}. The higher-energy component may be attributed to phonon/vibrational side-structure. In order to fit the $pheo_a$ bleach obtained in the presence of Q_AH_2, a broadening factor of ~1.5 was introduced for the $pheo_a$ that we assign to $Pheo_{D1}$.

From the analysis described above, it can be shown that, in the Q_A^--induced electrochromism, the entire $pheo_a$ Q_X band does not shift uniformly (Figure 7). The shift is predominantly of the band that contains the narrower component. The photoinduced bleaches in both the Q_AH_2 and Q_A^- states of PS II are also of this absorption band. For bleaches in the Q_A^- state, the EPR split signal shows that the active branch $pheo_a$ ($Pheo_{D1}$) is being reduced upon photoillumination. The similarity of the Q_X bleach in the Q_AH_2 state, except for an increase in the inhomogeneous broadening, suggests that the same $pheo_a$ is reduced by the illumination. This is a clear demonstration that it is the $Pheo_{D1}$ that is responsible for the well-known C550 shift, as expected.

Jankowiak et al.[41] modeled the $pheo_a$ Q_X absorbance in D1/D2/$cytb_{559}$ reaction centers (RC-5) using two Gaussians of approximately the same width and separated by ~90 cm^{-1}. Bleaching of the $pheo_a$ Q_X absorption via both chemical and photoinduced reductions was used to assign the lower-energy component to $Pheo_{D1}$. This phenomenology is consistent with our description of the $pheo_a$ Q_X absorption bands for the spinach core complex data (see above), where the average separation of the $Pheo_{D1}$ and $Pheo_{D2}$ excitations in the charge-neutral state (Q_AH_2) is ~70 cm^{-1}, and with $Pheo_{D1}$ appearing at lower energy. As absorbance features are known to broaden in D1/D2/$cytb_{559}$ reaction center preparations as compared to core complexes,[33] differences in the line shape of the $Pheo_{D1}$ excitation between these preparations are not surprising.

Q_Y $Pheo_{D1}$ Transition in PS II. As discussed in the Introduction, literature models propose two quite different positions for the dominant Q_Y $Pheo_{D1}$ excitation in PS II; either ~684 nm or ~672 nm. These two possibilities are discussed below within the context of the most recent crystallographic data,[15] which provide the relative positions and orientations of the reaction center pigments. There is little dispute that Chl_{D1} absorbs near 684 nm. EPR orientation studies[42] and more recently absorption spectra using site-directed mutants[43−45] have shown that the ^3P bleach is predominately localized on the Chl_{D1} pigment.

Assigning Q_Y $Pheo_{D1}$ at 684 nm. The Q_Y $Pheo_{D1}$ excitation has historically been assigned to ~684 nm, via the narrow bleach seen at this wavelength upon $Pheo_{D1}$ reduction and the electrochromic shift seen at a similar wavelength upon Q_A reduction (see Introduction). This assignment is however difficult to reconcile with the results presented in this work as it does not account for (i) the area of the apparent Q_Y bleach; (ii) the position of the apparent bleach in the Q_A^- state, relative to the Q_AH_2 state; and (iii) the highly structured CD change in the region of the bleach.

The area of the apparent Q_Y bleach at ~684 nm is significantly greater than that for a $pheo_a$, once calibrated against the area of the Q_X bleach. This result requires the "bleach" to be composite.[11] The "bleach" can also be associated with the negative edge of a blue shift on Chl_{D1}, appearing at ~684 nm, induced by the electric field of the reduced $Pheo_{D1}$.

Chl_{D1} is ~10 Å from the $Pheo_{D1}$.[15] The expected electrochromic shift on the Chl_{D1} upon $Pheo_{D1}$ reduction is 80 cm^{-1}, taking the orientation of $\Delta\mu_Y$ along the N_B-N_D axis[23] (IUPAC nomenclature[46]) and using a effective dielectric constant of $\varepsilon = 2$. This value is not significantly altered by rotating the $\Delta\mu_Y$ direction in the chlorin ring by ~15° in the direction of N_C as used in ref 14. This shift is greater than the line width of Chl_{D1}. If $Pheo_{D1}$ and Chl_{D1} both absorbed near 684 nm, the total "bleach" should correspond to the area of 1 chl_a and 1 $pheo_a$ combined, and consequently, ~2× larger than experimentally observed. Ascribing a smaller shift on Chl_{D1} to reduce the observed bleach area would require an unconventional orientation of its $\Delta\mu_Y$ (70−80° off the N_B-N_D axis toward N_C).

The position of the apparent bleach shifts to lower energy by ~10 cm^{-1} in the Q_AH_2 state as compared to the Q_A^- state. The expected position of the $Pheo_{D1}$ bleach in the Q_AH_2 state as compared to the Q_A^- state, again using crystallographically determined orientations of the $\Delta\mu$, now for $Pheo_{D1}$, is ~60 cm^{-1} to higher energy.[12−14] Thus, assigning the $Pheo_{D1}$ excitation at ~684 nm would require an unconventional $\Delta\mu_Y$ orientation for $Pheo_{D1}$ as well as an unconventional orientation of $\Delta\mu_Y$ for Chl_{D1}. An unconventional orientation for $\Delta\mu_Y$ of $Pheo_{D1}$ was proposed by Peterson Årsköld et al.[22]

The highly structured CD change associated with reduction of the $Pheo_{D1}$ observed in spinach places significant constraints on any description of the electronic structure of the reaction center pigment system. The $\Delta A/A$ of the CD features is of the order of ~10^{-3} and consequently an order of magnitude higher than normally associated with monomeric chl_a CD. Integration of the total CD change observed establishes that this CD difference is close to conservative. Both these observations suggest that the changes seen have an excitonic origin.

Importantly, the individual features in the CD difference spectrum seen in the region of the apparent Q_Y bleach are significantly narrower than any absorption (bleach) feature seen. Hence, the CD difference spectrum does not identify the position of a single excitation but instead indicates the overlap of excitations. The highly structured CD feature that coincides with the bleach must therefore arise from at least two exciton states near that position. Furthermore, these two exciton states must lie within each other's line width, (i.e., the exciton splitting between these two pigments cannot exceed ~25 cm^{-1}).

The structured CD change cannot be readily interpreted within a model where the $Pheo_{D1}$ excitation coincides with the bleach position (~684 nm). In such a model, the two overlapping exciton states giving rise to the structured CD change would be associated with $Pheo_{D1}$ and Chl_{D1}. Taking the conventional orientation of the transition dipole moments for the $Pheo_{D1}$ and Chl_{D1}, or even allowing them to vary by up to 20°, leads to an dipole−dipole coupling of 50−70 cm^{-1}. This estimate of coupling is reduced by using a transition monopole method but remains at ~45−55 cm^{-1}.[14,23−25] This value is ~2× the maximal coupling allowable from the nature of the observed CD changes upon $Pheo_{D1}$ reduction. Hence, assigning the $Pheo_{D1}$ excitation to be at 684 nm would also require the transition dipole orientations of $Pheo_{D1}$ or Chl_{D1} (or both) to be unconventional.

Assigning Q_Y of $Pheo_{D1}$ at 672 nm. The data presented in this paper are consistent with the dominant $Pheo_{D1}$ excitation being at ~672 nm. Following the basic assignments of Renger and co-workers, our modeling suggests that the exciton state at 683.6 nm that is responsible for the apparent Q_Y bleach is dominated by the accessory Chl_{D1}. Upon reduction of $Pheo_{D1}$ the "Chl_{D1} exciton" shifts to the blue. The negative edge of this shift appears then as a bleach.

The integrated intensity of the apparent Q_Y bleach at 683.8 nm is consistent with it being the loss of a chlorophyll, as opposed to the loss of a $pheo_a$ (oscillator strength is ~0.7 chl_a[38]).

The electrochromic shift on Chl_{D1} induced by the reduction of Q_A is calculated to be relatively small. This is consistent with experimental observations[22] of a value of ~10 cm^{-1}. The apparent Q_Y bleach positions in the Q_A^- and Q_AH_2 systems are different by ~10 cm^{-1} as is seen in the double-difference spectra, again consistent with its assignment to Chl_{D1}.

Our simulations (discussed below) show that the assignment of the apparent Q_Y bleach as a shift on the Chl_{D1} pigment is also consistent with the CD changes observed. Within the model of Raszewski et al.,[14,23] the exciton states involved in this CD change involve a dominantly Chl_{D1} state along with a dominantly $Pheo_{D2}$ state. Evidence for such a $Pheo_{D2}$ assignment in D1/D2/$cytb_{559}$ reaction centers comes from experiments where $Pheo_{D2}$ was substituted by a chemically modified pheophytin which absorbed well to the blue of $pheo_a$. This led to a loss of absorption at ~680 nm.[47] Significant CD changes were also observed at ~680 nm upon $Pheo_{D2}$ replacement.

Within this scheme, the CD difference feature we observed can be understood (see below). The highly structured pattern arises from changes in the CD of two exciton states (as discussed above), one dominated by Chl_{D1} and the other by $Pheo_{D2}$. Indeed, $Pheo_{D2}$ is the only inner reaction center pigment to which Chl_{D1} does not strongly couple. Estimates for the coupling between these two pigments are ~3 cm^{-1} and thus less than the ~25 cm^{-1} upper limit required for it to be consistent with the CD data.

Simultaneous Simulation of the CD Changes and Q_Y Absorption Bleach Data. Simple exciton calculations were undertaken, for the PS II originating from different species, to simultaneously fit the CD difference and absorption difference spectra upon $Pheo_{D1}$ reduction (see the Materials and Methods and Supporting Information s5). Our simulation of the absorption bleach upon $Pheo_{D1}$ reduction in PS II cores from spinach (dark Q_AH_2 state) is shown in Figure 8. As described above, the negative edge of a large blue shift on the Chl_{D1} (30−50 cm^{-1}) defines the bleach position. The $Pheo_{D1}$ bleach position is now inferred to appear at ~672 nm. This position is close to the corresponding feature in D1/D2/$cytb_{559}$. The positive feature at ~680 nm is also associated with the Chl_{D1} blue shift, although the asymmetry of the band is not accounted for very well in the modeling. The analysis does not include the appearance of a $Pheo_{D1}$ anion, known to appear to absorb to the blue of the neutral species.[9] The pigment contributions to each of the exciton states is shown in Supporting Information s6.

The simulated CD difference spectrum is also shown in Figure 8. The structured CD change (in the region of the bleach at 684 nm) arises from the spectral overlap of the $Pheo_{D2}$ and Chl_{D1} exciton states. In the dark (Q_AH_2) state, the "dominantly Chl_{D1}" exciton appears at ~683.5 nm and the "dominantly $Pheo_{D2}$" exciton at ~685 nm (Figure 8D). The two exciton states have oppositely signed CD with approximately the same CD intensity. Upon $Pheo_{D1}$ reduction, the site energy for Chl_{D1} shifts 30−50 cm^{-1} to the blue. Thus, the exciton states shift apart, appearing at ~681 nm (Chl_{D1}) and ~685 nm ($Pheo_{D2}$) (Figure 8E). The subtraction of these two sets of two bands leads to the narrow structured CD change seen (Figure 8F). Its overall structure can be described as follows. The "$Pheo_{D2}$ exciton" is responsible for the red-most turning point, whereas the electrochromically shifting "Chl_{D1} exciton" is responsible for the other two CD turning points of the structured CD change. The CD difference spectrum in blue region (665−680 nm) is also well-simulated. These changes correspond to the reduction of intensity of a "dominantly $Pheo_{D1}$" exciton that has a negative sign.

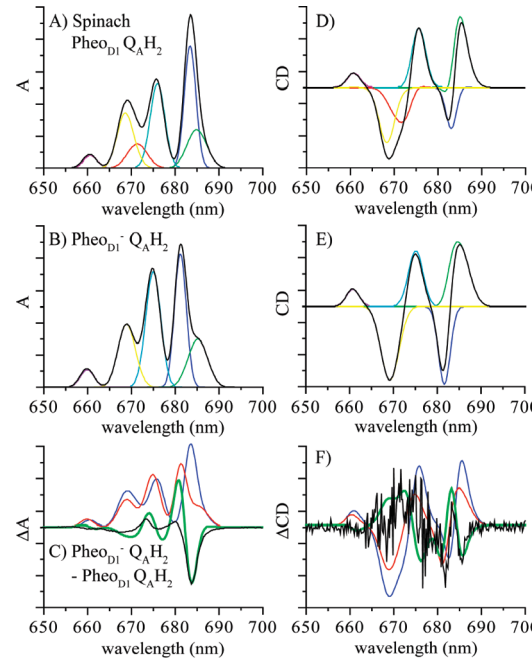

Figure 8. Fit of the light-minus-dark absorption difference and CD change observed upon photoaccumulation of the $Pheo_{D1}^-$ in spinach poised in the Q_AH_2 state in the dark (from Figures 3B(b), 6A(b)). Panel A: Positions of the six absorption (exciton) bands in the Q_AH_2 state. Panel B: Positions of the five remaining absorption bands after the bleach of the $Pheo_{D1}$. Panel C: Simulation of the light-minus-dark absorption difference. Panel D: Positions of the six CD bands in the Q_AH_2 state. Panel E: Positions of the five remaining CD bands after the bleach of the $Pheo_{D1}$. Panel F: Simulation of the light-minus-dark CD difference. Color coding for panels A, B, D, E: black, theoretical absorption/CD spectrum; blue, Chl_{D1} absorbance/ CD band; red, $Pheo_{D1}$ absorbance/CD band; green, $Pheo_{D2}$ absorbance/CD band; cyan + pink, P_{D1}, P_{D2} absorbance/CD bands; yellow, Chl_{D2} absorbance/CD band. Color coding for panels C and F: black, data, absorbance/CD difference; blue, dark $Pheo_{D1}Q_AH_2$ state; red, light $Pheo_{D1}^-Q_AH_2$ state; green, simulation of absorbance/CD difference (i.e., red trace − blue trace).

$Pheo_{D2}$ has been one of the least experimentally accessible pigments in the PS II core complexes. Its assignment to ~680 nm by Raszewski et al. is simply inferred from its position in D1/D2/$cytb_{559}$. No experimental data have been available to directly probe the position of the $Pheo_{D2}$ in core complexes. The position and orientation of $Pheo_{D2}$ ensure that it is relatively insensitive to electrochromic effects associated with Q_A- and $Pheo_{D1}^-$. Upon addition, a spectral shift of the site energy of $Pheo_{D2}$ to the red will have a smaller influence on the exciton states than similar changes for the other five pigments. $Pheo_{D2}$ only couples significantly to Chl_{D2} and in the Raszewski et al. model; their site energies are separated by ~200 cm^{-1}.

Our overall assignments are consistent with those of Raszewski et al.[14,23] with the exception of the placement of $Pheo_{D2}$. The assignment of the "$Pheo_{D2}$ exciton" to ~685 nm represents a shift to lower energy of ~100 cm^{-1} compared to its position in D1/D2/$cytb_{559}$. The highly structured CD changes seen upon $Pheo_{D1}$ reduction in PS II core complexes presented in this work closely constrain the position of the $Pheo_{D2}$ exciton in intact PS II core complex preparations. This then points to a significant spectral shift of its position compared to that observed in isolated D1/D2/$cytb_{559}$ preparations. It is noted that in the model of Raszewski et al.[14,44,45] a similar shift in the site energy of the Chl_{D1} between core complexes and isolated D1/D2/cyt_{b559} reaction centers was required. A more definitive assignment of the "$Pheo_{D2}$ exciton" based on our data may require a more

rigorous treatment of the homogeneous line shapes of the pigment transitions.

Species Comparison of Absorption Difference Spectra. Changes in the hydrogen bonding from the protein to the 13^1 keto of the $Pheo_{D1}$ in PS II[17] and the $BPheo_L$ in the BRC[16,18] have been shown to affect the pigment site energy. In the wild-type BRC, L-Glu104 provides a hydrogen bond to the $BPheo_L$ 13^1 keto, while in *Synechocystis*, the corresponding residue is D1-Gln130, which does not provide a hydrogen bond for the $Pheo_{D1}$ 13^1 keto.

In the BRC and *Synechocystis* systems, mutants have been created that target these residues so as to remove or add a hydrogen bond, respectively. In both systems, it was shown that a hydrogen bond to the (B)$Pheo_{D1(L)}$ 13^1 keto results in a red-shifted Q_X band.[16−18] In the BRC, the $BPheo_L$ Q_Y band is blue-shifted due to the hydrogen bond,[18] while in *Synechocystis*, the dominant Q_Y electrochromic feature is red-shifted.[17]

Synechocystis, *T. vulcanus*, and higher plants differ in their D1 polypeptide sequence in the region where $Pheo_{D1}$ is bound. In higher plants, there is a Glu at position D1−130, while the corresponding residue in *T. vulcanus* and *Synechocystis* is D1-Gln130, at least under normal growth conditions.[48] Consequently, the $Pheo_{D1}$ Q_X band in higher plants is 2.5 nm to the red as compared to either *Synechocystis*[17] or *T. vulcanus*,[49] as determined by the C550 electrochromic shift and the position of the bleach (see Figure 5).

Within the model presented above,[14,23] the apparent bleach in Q_Y is assigned to a shift on the Chl_{D1}. Our calculations establish that a ~50 cm^{-1} shift of a $Pheo_{D1}$ pigment centered at ~672 nm has a minimal influence on the transition energy of the Chl_{D1} exciton (~2 cm^{-1}). Thus, a change in the Q_Y bleach position between organisms indicates a variation in the mean site energy distribution of the Chl_{D1} rather than $Pheo_{D1}$.

Species Comparison of CD Difference Spectra. The CD difference spectrum in *Synechocystis* can be rationalized in the same way as for spinach (see Figures 8 and 9). The absorption band for the Chl_{D1} in this organism shifts to the blue as compared to spinach, as evidenced by the apparent Q_Y bleach. Consequently, there is less overlap of the $Pheo_{D2}$ and Chl_{D1} "exciton bands", leading to a broader CD pattern. The transition energy of the accessory Chl_{D1} in *Synechocystis* is close to that seen for D1/D2/cytb_{559} preparations, as monitored by the triplet bleach position.[44,45,50] To fit the CD change, the position of the Q_Y $Pheo_{D1}$ pigment had to be shifted to the red. This is in accord with the expected electrochromism that is induced due to the presence of Q_A^-. Arguably, the CD fitting in *Synechocystis* is significantly better than that for spinach; it provides a better fit to the structured CD change at the position of the bleach (Figure 9F). This is perhaps not surprising, as the crystallographic data that was used as the basis for these simulations comes from cyanobacterial sources, not higher plants.

The CD difference as seen in *T. vulcanus* is most likely a photophysical effect associated with illumination-induced changes of the proximal light-harvesting complexes CP43 and CP47. The Q_Y CD changes seen are virtually lost upon annealing at 90 K with a corresponding ~50% decrease in $Pheo_{D1}^-$ as estimated by the Q_X bleach. The CD changes seen are similar to the photophysical CD changes observed in isolated spinach CP43 antennae complexes,[36] except red-shifted. The narrow long-wavelength absorption of CP43 in *T. elongatus,* an organism very similar to *T. vulcanus,* is red-shifted as compared to spinach.[51] The negative CD feature in *T. vulcanus* core complexes, which is at least partly associated with CP43, appears at 684.8 nm, compared to 683.3 nm for the corresponding feature in spinach core complexes.

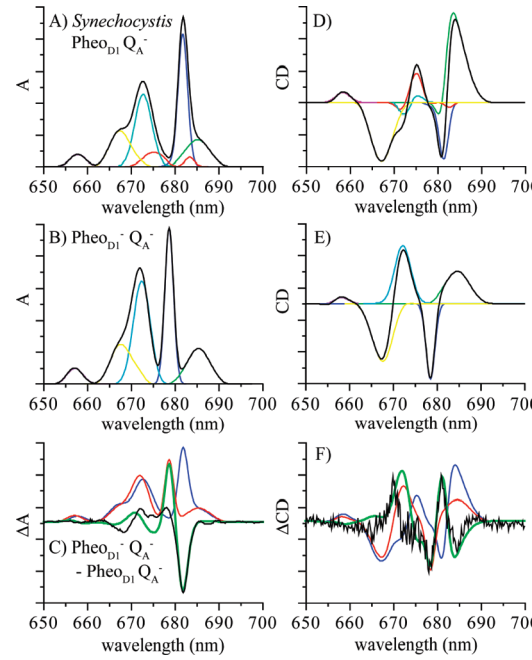

Figure 9. Fit of light-minus-dark spectra in *Synechocystis* PS II cores poised in the Q_A^- in the Q_Y region (see text). Panel A: Positions of the six absorption (exciton) bands in the Q_A^- state. Panel B: Positions of the five remaining absorption bands after the bleach of the $Pheo_{D1}$. Panel C: Simulation of the light-minus-dark absorption difference. Panel D: Positions of the 6 CD bands in the Q_A^- state. Panel E: Positions of the five remaining CD bands after the bleach of the $Pheo_{D1}$. Panel F: Simulation of the light-minus-dark CD difference. Color coding for panels A−F are exactly the same as Figure 8.

As most of the illumination-induced CD changes in *T. vulcanus* are associated with photophysical rather than photochemical changes, modeling becomes problematic. Unlike the other species studied, the lowest energy CD difference feature in *T. vulcanus* is positively signed. Within the model described, the lowest energy CD difference feature is associated with the dark state (prior to $Pheo_{D1}$ reduction) for *T. vulcanus* is the Chl_{D1} exciton. This exciton band must have a positive CD sign, and thus, the red-most CD difference feature should be negative and not positive. When a scaled subtraction of the CP43 photophysical CD change is made, the remnant CD change is within the noise and 2−3 times smaller in amplitude than the corresponding change seen in spinach. This small amplitude is consistent with our modeling for *T. vulcanus*, where a significant red shift of the dominantly Chl_{D1} exciton, relative to its position in other organisms, leads to a decrease in its CD intensity.

Reaction Center of PS II. Frese et al.[52] reported an anomalously large Stark signal for the $Pheo_{D1}$ Q_X band in D1/D2/cytb_{559} preparations, as well as nonclassical Stark behavior in the long-wavelength Q_Y region. In BRC mutants, it has also been suggested[53] that a classic Liptay-type analysis may be inadequate to describe the Stark spectra. Deviations from the typical Liptay line shape behavior in Stark spectra have been predicted when there is mixing of the states involved in the observed transition with one (or more) other states.[53] The mixing of pigment transitions with charge transfer states has been featured in these discussions of non-Liptay Stark behavior.[52,53] Such considerations may be required to further our understanding of the Q_A^- and $Pheo_{D1}^-$-induced electrochromism in PS II.

TABLE 2: Simulated Absorption/CD Band Positions for Spinach (Q_AH_2) and *Synechocystis* (Q_A^-)[a]

	mean site energy distribution (nm)		absorbance/CD bands (nm)	
	Spinach (Q_AH_2)	*Synechocystis* (Q_A^-)	Spinach (Q_AH_2)	*Synechocystis* (Q_A^-)
Chl_{D1}	682.5 ± 0.1	680.0 ± 0.1	683.6 ± 0.1	681.7 ± 0.1
$Pheo_{D2}$	685 ± 0.5	685 ± 0.5	~685	~685
$Pheo_{D1}$	672 ± 0.5	677 ± 0.5	~672	~675
P_{D1}	668.5 ± 0.5	666 ± 0.5	~676	~673
P_{D2}	669.5 ± 0.5	666 ± 0.5	~660	~658
Chl_{D2}	668 ± 0.5	677 ± 0.5	~669	~667

[a] See Figures 8 and 9.

Novoderezhkin et al.[24,25] include charge transfer states in their modeling of PS II optical spectra and incorporate Stark data. However, they do not address Q_A^--induced electrochromism or $Pheo_{D1}^-$ photoaccumulation data. As discussed above, Raszewski et al.[14,23] do address the latter data, but do not include charge transfer states in their model or Stark data. A significant advancement of our understanding of the electronic structure of the PSII reaction center may arise from an integration of the current theoretical approaches and the new experimental data presented here.

It seems appropriate that charge transfer states and subsequent charge transfer character of pigment excitations be incorporated in any modeling of electrochromic effects in PS II core complexes. Such an approach may also help reconcile the marked difference in electrochromic effects between PS II and BRC. Highlighted is the large electrochromic shift on the Q_X band of $Pheo_{D1}$ upon Q_A^- formation in PSII compared to the barely measurable electrochromic shift of the $BPheo_L$ Q_X transition in the BRC.[20]

Summary

Low-temperature absorption and structured CD changes associated with the photo-accumulation of $Pheo_{D1}^-$ in intact PS II core complexes provide new evidence for the assignment of the reaction center pigments. These results are shown to be consistent with the overall assignments of Raszewski et al.[14,23] which place the dominant $Pheo_{D1}$ excitation near 672 nm.

The highly structured CD changes seen upon $Pheo_{D1}$ reduction in PS II core complexes presented in this work closely constrains the position of the $Pheo_{D2}$ exciton in intact PS II core complex preparations. Simple exciton calculations point to a significant spectral shift of this pigment when compared to that observed in isolated D1/D2/cyt_{b559} preparations.

Acknowledgment. The authors are grateful to Mr. K. Jackman for invaluable technical assistance and acknowledge support from the Australian Research Council (DP 0665718) and a joint French-Australian Science and Technology (FAST) Programme (Australian DEST grant number FR07001). JLH and AWR were supported in part by EU/Energy project SOLAR-H2 (contract # 212508). The authors would also like to thank Profs. R. Debus and J.-R. Shen for providing *Synechocystis* and *T. vulcanus* core complexes used in this work.

Supporting Information Available: Additional material detailing optical control measurements, additional data from room temperature bleaching experiments, EPR controls, and a further description of the model given in the text. This material is available free of charge via the Internet at http://pubs.acs.org.

References and Notes

(1) Diner, B. A.; Rappaport, F. *Annu Rev Plant Biol.* **2002**, *53*, 551.
(2) Rutherford, A. W.; Zimmermann, J. L. *Biochim. Biophys. Acta* **1984**, *767*, 168.
(3) Klimov, V. V.; Dolan, E.; Shaw, E. R.; Ke, B. *Proc. Natl. Acad. Sci. U.S.A.* **1980**, *77*, 7227.
(4) Klimov, V. V.; Dolan, E.; Ke, B. *FEBS Lett.* **1980**, *112*, 97.
(5) van Mieghem, F. J. E.; Nitschke, W.; Mathis, P.; Rutherford, A. W. *Biochim. Biophys. Acta* **1989**, *977*, 207.
(6) Deligiannakis, Y.; Hanley, J.; Rutherford, A. W. *Biochemistry* **1998**, *37*, 3329.
(7) van Mieghem, F.; Brettel, K.; Hillman, B.; Kamlowski, A.; Rutherford, A. W.; Schlodder, E. *Biochemistry* **1995**, *34*, 4798.
(8) Klimov, V. V.; Klevanik, A. V.; Shuvalov, V. A.; Krasnovsky, A. A. *FEBS Lett.* **1977**, *82*, 183.
(9) Fujita, I.; Davis, M. S.; Fajer, J. *J. Am. Chem. Soc.* **1978**, *100*, 6280.
(10) van Gorkom, H. J. *Biochim. Biophys. Acta* **1974**, *347*, 439.
(11) Ganago, I. B.; Klimov, V. V.; Ganago, A. O.; Shuvalov, V. A.; Erokhin, Y. E. *FEBS Lett.* **1982**, *140*, 127.
(12) Krawczyk, S. *Biochim. Biophys. Acta* **1991**, *1056*, 64.
(13) Mulkidjanian, A. Y.; Cherepanov, D. A.; Haumann, M.; Junge, W. *Biochemistry* **1996**, *35*, 3093.
(14) Raszewski, G.; Diner, B. A.; Schlodder, E.; Renger, T. *Biophys. J.* **2008**, *95*, 105.
(15) Loll, B.; Kern, J.; Saenger, W.; Zouni, A.; Biesiadka, J. *Nature* **2005**, *438*, 1040.
(16) Bylina, E. J.; Kirmaier, C.; McDowell, L.; Holten, D.; Youvan, D. C. *Nature* **1988**, *336*, 182.
(17) Stewart, D. H.; Nixon, P. J.; Diner, B. A.; Brudvig, G. W. *Biochemistry* **2000**, *39*, 14583.
(18) Breton, J.; Bylina, E. J.; Youvan, D. C. *Biochemistry* **1989**, *28*, 6423.
(19) Steffen, M. A.; Lao, K.; Boxer, S. G. *Science* **1994**, *264*, 810.
(20) Chuang, J. I.; Boxer, S. G.; Holten, D.; Kirmaier, C. *Biochemistry* **2006**, *45*, 3845.
(21) van Gorkom, H. J.; Tamminga, J. J.; Haveman, J. *Biochim. Biophys. Acta* **1974**, *347*, 417.
(22) Peterson Årsköld, S.; Masters, V. M.; Prince, B. J.; Smith, P. J.; Pace, R. J.; Krausz, E. *J. Am. Chem. Soc.* **2003**, *125*, 13063.
(23) Raszewski, G.; Saenger, W.; Renger, T. *Biophys. J.* **2005**, *88*, 986.
(24) Novoderezhkin, V. I.; Dekker, J. P.; van Grondelle, R. *Biophys. J.* **2007**, *93*, 1293.
(25) Novoderezhkin, V. I.; Andrizhiyevskaya, E. G.; Dekker, J. P.; van Grondelle, R. *Biophys. J.* **2005**, *89*, 1464.
(26) Kamiya, N.; Shen, J.-R. *Proc. Natl. Acad. Sci. U.S.A.* **2003**, *100*, 98.
(27) Smith, P. J.; Peterson, S.; Masters, V. M.; Wydrzynski, T.; Styring, S.; Krausz, E.; Pace, R. J. *Biochemistry* **2002**, *41*, 1981.
(28) Debus, R. J.; Strickler, M. A.; Walker, L. M.; Hillier, W. *Biochemistry* **2005**, *44*, 1367.
(29) Shen, J.-R.; Ikeuchi, M.; Inoue, Y. *FEBS Lett.* **1992**, *301*, 145.
(30) Shen, J. R.; Inoue, Y. *Biochemistry* **1993**, *32*, 1825.
(31) Hughes, J. L.; Krausz, E. Electronic Spectroscopy. In *Applications of Physical Methods to Inorganic and Bioinorganic Chemistry*, 2nd ed.; Scott, R. A., Lukehart, C. M., Eds.; John Wiley & Sons, Ltd.: New York, 2007; p 79.
(32) Stranger, R.; Dubicki, L.; Krausz, E. *Inorg. Chem.* **1996**, *35*, 4218.
(33) Krausz, E.; Cox, N.; Årsköld, S. *Photosynth. Res.* **2008**, *98*, 207.
(34) Stewart, D. H.; Brudvig, G. W. *Biochim. Biophys. Acta* **1998**, *1367*, 63.
(35) Hughes, J. L.; Picorel, R.; Seibert, M.; Krausz, E. *Biochemistry* **2006**, *45*, 12345.
(36) Hughes, J. L.; Prince, B. J.; Peterson Årsköld, S.; Krausz, E.; Pace, R. J.; Picorel, R.; Seibert, M. *J. Lumin.* **2004**, *108*, 131.
(37) Okamura, M. Y.; Isaacson, R. A.; Feher, G. *Biochim. Biophys. Acta* **1979**, *546*, 394.
(38) Houssier, C.; Sauer, K. *J. Am. Chem. Soc.* **1970**, *92*, 779.
(39) Rutherford, A. W.; Paterson, D. R.; Mullet, J. E. *Biochim. Biophys. Acta* **1981**, *635*, 205.
(40) Vacha, F.; Durchan, M.; Siffel, P. *Biochim. Biophys. Acta* **2002**, *1554*, 147.
(41) Jankowiak, R.; Rätsep, M.; Picorel, R.; Seibert, M.; Small, G. J. *J. Phys. Chem. B* **1999**, *103*, 9759.
(42) van Mieghem, F. J. E.; Satoh, K.; Rutherford, A. W. *Biochim. Biophys. Acta* **1991**, *1058*, 379.
(43) Diner, B. A.; Schlodder, E.; Nixon, P. J.; Coleman, W. J.; Rappaport, F.; Lavergne, J.; Vermaas, W. F. J.; Chisholm, D. A. *Biochemistry* **2001**, *40*, 9265.
(44) Schlodder, E.; Coleman, W. J.; Nixon, P. J.; Cohen, R. O.; Renger, T.; Diner, B. A. *Philos. Trans. R. Soc. London [Biol.]* **2008**, *363*, 1197.

(45) Schlodder, E.; Renger, T.; Raszewski, G.; Coleman, W. J.; Nixon, P. J.; Cohen, R. O.; Diner, B. A. *Biochemistry* **2008**.

(46) Moss, G. *Eur. J. Biochem.* **1988**, 178.

(47) Germano, M.; Shkuropatov, A. Y.; Permentier, H.; de Wijn, R.; Hoff, A. J.; Shuvalov, V. A.; van Gorkom, H. J. *Biochemistry* **2001**, *40*, 11472.

(48) Garczarek, L.; Dufresne, A.; Blot, N.; Cockshutt, A. M.; Peyrat, A.; Campbell, D. A.; Joubin, L.; Six, C. *ISME J.* **2008**, *2*, 937.

(49) Peterson Årsköld, S.; Smith, P. J.; Shen, J.-R.; Pace, R. J.; Krausz, E. *Photosynth. Res.* **2005**, *84*, 309.

(50) Hillmann, B.; Brettel, K.; van Mieghem, F.; Kamlowski, A.; Rutherford, A. W.; Schlodder, E. *Biochemistry* **1995**, *34*, 4814.

(51) Breton, J.; Katoh, S. *Biochim. Biophys. Acta* **1987**, *892*, 99.

(52) Frese, R. N.; Germano, M.; de Weerd, F. L.; van Stokkum, I. H. M.; Shkuropatov, A. Y.; Shuvalov, V. A.; van Gorkom, H. J.; van Grondelle, R.; Dekker, J. P. *Biochemistry* **2003**, *42*, 9205.

(53) Moore, L. J.; Zhou, H.; Boxer, S. G. *Biochemistry* **1999**, *38,* 11949.

(54) Renger, T. *Phys. Rev. Lett.* **2004**, *93*, 188101.

(55) Hughes, J. L.; Smith, P.; Pace, R.; Krausz, E. *Biochim. Biophys. Acta* **2006**, *1757*, 841.

JP808796X